

Geophysical Research Letters®



RESEARCH LETTER

10.1029/2022GL098946

Key Points:

- Atmospheric pressure fluctuations on Mars can produce significant methane seepage from potentially habitable depths (up to 200 m)
- Modeled surface methane seepage patterns are highly seasonal and coincide with rover measurements of elevated concentrations at Gale crater
- Magnitude and timing of modeled surface flux is comparable to existing plume estimates, supporting a model of localized surface releases

Supporting Information:

Supporting Information may be found in the online version of this article.

Correspondence to:

J. P. Ortiz,
jportiz@lanl.gov

Citation:

Ortiz, J. P., Rajaram, H., Stauffer, P. H., Harp, D. R., Wiens, R. C., & Lewis, K. W. (2022). Barometric pumping through fractured rock: A mechanism for venting deep methane to Mars' atmosphere. *Geophysical Research Letters*, 49, e2022GL098946. <https://doi.org/10.1029/2022GL098946>

Received 30 MAR 2022

Accepted 26 JUN 2022

Author Contributions:

Conceptualization: J. P. Ortiz, H. Rajaram, R. C. Wiens, K. W. Lewis

Data curation: J. P. Ortiz

Funding acquisition: J. P. Ortiz, H. Rajaram, P. H. Stauffer, D. R. Harp

Investigation: J. P. Ortiz

Methodology: J. P. Ortiz, H. Rajaram

Resources: R. C. Wiens, K. W. Lewis

Software: J. P. Ortiz, P. H. Stauffer, D. R. Harp

Supervision: H. Rajaram, P. H. Stauffer

Validation: J. P. Ortiz

Visualization: J. P. Ortiz

© 2022. The Authors.

This is an open access article under the terms of the [Creative Commons Attribution License](https://creativecommons.org/licenses/by/4.0/), which permits use, distribution and reproduction in any medium, provided the original work is properly cited.

Barometric Pumping Through Fractured Rock: A Mechanism for Venting Deep Methane to Mars' Atmosphere

J. P. Ortiz^{1,2} , H. Rajaram² , P. H. Stauffer¹ , D. R. Harp^{1,3} , R. C. Wiens^{4,5} , and K. W. Lewis⁶ 

¹Computational Earth Science, Los Alamos National Laboratory, Los Alamos, NM, USA, ²Department of Environmental Health and Engineering, The Johns Hopkins University, Baltimore, MD, USA, ³Now at Science and Analytics Team, The Freshwater Trust, Portland, OR, USA, ⁴Space and Remote Sensing, Los Alamos National Laboratory, Los Alamos, NM, USA, ⁵Now at Earth, Atmospheric, and Planetary Sciences, Purdue University, West Lafayette, IN, USA, ⁶Department of Earth and Planetary Sciences, The Johns Hopkins University, Baltimore, MD, USA

Abstract Both the source of methane on Mars and the mechanism for transmission from the subsurface to the atmosphere are not fully understood. Previous seepage simulations have invoked relatively shallow subsurface sources to explain observed methane signatures on Mars. We propose that barometric-pressure pumping through fracture networks could be an effective mechanism for methane transport from the deep subsurface on Mars. Using atmospheric pressure data gathered by *Curiosity* as input, we simulate methane gas transport from depths of 200 m to the surface. Even with such a deep source, our model reproduces the observed seasonality of methane, and the simulated surface methane fluxes fall within the range of previous estimates derived from atmospheric observations. Because 200 m is the likely minimum hospitable depth for living methanogenic microbes, our fracture network model indirectly reinvestigates the possibility of a microbial source of methane on Mars.

Plain Language Summary The existence of methane on Mars is a topic of significant interest because of its potential association with subsurface microbial life. Measurements of methane in the atmosphere of Mars indicate that its abundance fluctuates over time. Although the source of methane is unknown, it most likely comes from below the surface of Mars; however, the range of depths of potential methane sources is not well constrained. If methane is currently being produced by living microbes, it would have to be at depths of at least 200 m in order to support life. Nearly all prior modeling work in this area has considered relatively slow, inefficient methane transport mechanisms, which limits the methane sources to the shallow martian subsurface. In this paper, we describe and model a mechanism capable of transporting significant quantities of methane to the atmosphere from depths capable of supporting living methane-producing microorganisms. We also find that the methane seepage pattern generated by our model is highly seasonal, and closely follows the pattern of atmospheric methane concentrations measured by the *Curiosity* rover.

1. Introduction

One of the biggest questions motivating the exploration of Mars is whether the planet supports or ever supported life, and it is for this reason that the potential link between methane occurrence and microbial life has garnered exceptional interest. Although there have been numerous reports of methane in Mars' atmosphere (Formisano et al., 2004; Giuranna et al., 2019; Krasnopolsky et al., 2004; Moores, King et al., 2019; Mumma et al., 2009), there is an ongoing debate about the occurrence of methane and the validity of such detections (Korablev et al., 2019; Villanueva et al., 2013; Webster et al., 2015; Zahnle et al., 2011). Currently, both the source of the methane and mechanism for its transmission to the atmosphere remain unknown. Seasonal variability in detected atmospheric methane abundance (Giuranna et al., 2019; Roos-Serote et al., 2016; Webster et al., 2018) coupled with the fact that methane has a relatively short lifetime in the martian atmosphere (Lefèvre & Forget, 2009) points toward active methane sources in the martian subsurface (Figure 1).

Most previous computational studies of subsurface methane transport on Mars have not explicitly considered rapid transport mechanisms such as advection, instead favoring diffusion (Moores, King et al., 2019; Stevens et al., 2015; Temel et al., 2019), which is much slower and only capable of transporting significant quantities of methane from relatively shallow depths. Most previous numerical studies of methane release from the martian

Writing – original draft: J. P. Ortiz, H. Rajaram
Writing – review & editing: J. P. Ortiz, H. Rajaram, P. H. Stauffer, D. R. Harp, R. C. Wiens, K. W. Lewis

subsurface have therefore focused on relatively shallow sources (~10–30 m depth) in order to explain short-term variations in atmospheric abundance, or else require relatively fast-acting destruction processes such as biological oxidation (Stevens et al., 2017). Such conclusions emphasizing shallow sources have implicitly ruled out extant methanogens because the depths habitable for martian microbes are estimated to be at least 200 m (Section 1 in Supporting Information S1).

Recent work by Viúdez-Moreiras et al. (2020) did examine advective fluxes caused by transient atmospheric pressure fluctuations, but the analysis emphasized relatively shallow methane sources (<10 m). That research was the first to evaluate the relevance of advective fluxes of methane to Mars' atmosphere, concluding that barometric pumping—an advective transport mechanism driven by atmospheric pressure fluctuations—could not significantly enhance regolith emissions past the first few meters of depth. However, the subsurface in that model was represented as a porous medium rather than a fractured porous medium. Fractures are critical to the transport of subsurface gases because they provide conduits through rock via well-connected high-permeability pathways (Buckingham, 1904; Nilson et al., 1991) with apertures (i.e., width of opening) much larger than pore diameters in porous rock, and should therefore be explicitly accounted for in advective gas transport models.

Evidence suggests that the martian subsurface is heavily fractured, with many fractures and faults believed to extend to depths >1 km (De Toffoli et al., 2018; Kronyak et al., 2019; Oehler & Etiopie, 2017; Rodríguez et al., 2005). Recent InSight data indicate that Mars' crustal density is substantially less than expected, suggesting high average porosity and extensive fracturing (Knapmeyer-Endrun et al., 2021; Lognonné et al., 2020). Furthermore, the lower gravitational force on Mars (~0.37 g_{Earth}) leads to lower lithostatic pressures than on Earth, which will result in higher fracture density and larger apertures at any depth (Heap et al., 2017), in turn leading to more efficient advective transport (Section 4.3 in Supporting Information S1).

On Earth, transport of deeply-sourced gases to the atmosphere can be greatly enhanced by barometric pumping. This mechanism has been studied extensively in terrestrial applications, such as: CO₂ leakage from carbon sequestration sites (Carroll et al., 2014; Dempsey et al., 2014; Pan et al., 2011; H. S. Viswanathan et al., 2008) and deep geological stores (Etiopie & Martinelli, 2002; Rey et al., 2014), methane leakage from hydraulic fracturing operations (Myers, 2012), radon gas entry into buildings (Tsang & Narasimhan, 1992), contaminant monitoring (Stauffer et al., 2018, 2019), and radionuclide gas seepage from underground nuclear explosions and waste storage facilities (Bourret et al., 2019, 2020; Carrigan et al., 1996, 1997; Harp et al., 2020; Jordan et al., 2014, 2015; Sun & Carrigan, 2014). Barometric highs in Earth's atmosphere push gases deeper into fractured rock, while barometric lows pull gases upward (Auer et al., 1996; Harp et al., 2018; Neeper, 2002, 2003). Because some of the gas molecules pulled upward subsequently diffuse from the fractures into the surrounding, relatively low-permeability rock matrix—in which the barometric pressure fluctuations do not propagate efficiently—a certain portion are not pushed back into the deeper subsurface during barometric highs. These molecules can diffuse back into the fracture and be available for upward transport during subsequent barometric lows. Over multiple cycles of atmospheric pressure variations, this fracture-matrix exchange produces a ratcheting mechanism that greatly enhances upward gas transport (Massmann & Farrier, 1992; Neeper & Stauffer, 2012a; Nilson et al., 1991; Takle et al., 2004). Etiopie and Oehler (2019) proposed that barometric pumping could be an effective transport mechanism for methane on Mars.

In this paper, we demonstrate the viability of the barometric-pumping transport mechanism for bringing deeply sourced methane to Mars' atmosphere based on a fractured rock representation of the martian subsurface. We present a model of subsurface flow and transport in fractured rock driven by measured martian atmospheric pressure fluctuations. To our knowledge, this is the first study to use fractured-rock flow and transport models to interrogate martian methane seepage. Our simulations confirm the ability of martian barometric fluctuations to promote surface seepage of significant quantities of methane from depths of up to 200 m, potentially reinvigorating support for the hypothesis that geologically deep, biogenically-produced methane could be the source of atmospheric methane on Mars. Our model also produces surface methane flux patterns consistent with seasonality in methane abundance observed at Gale crater. Combining the results of this modeling with current and future observations of trace gas release will allow us to draw links between active processes in the martian crust and gases detected in the atmosphere. By improving our understanding of methane transport mechanisms on Mars and their role in producing the observed methane episodicity, this work will facilitate evaluation of optimal targets and timing for both atmospheric detection (e.g., *Curiosity*) and shallow subsurface (e.g., *Perseverance*) isotopic fingerprinting upon eventual sample retrieval.

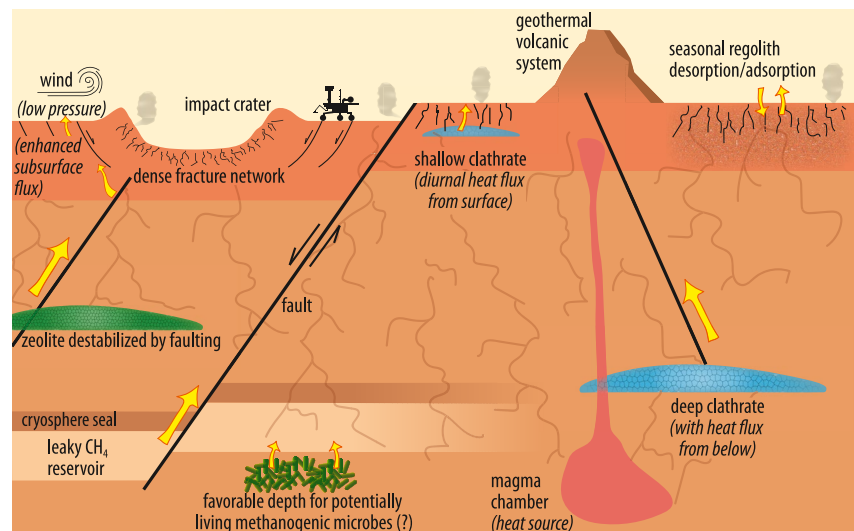


Figure 1. Conceptual diagram illustrating possible methane sources and release mechanisms in the martian subsurface. Features not to scale; spatial relationship between methane sources is designed to show that living biotic sources cannot be shallow. All sources shown, except regolith desorption, can be located at greater depths than those shown.

2. Methods: Fractured Rock Flow and Transport Simulations

We used the fractured-rock flow and transport simulations to (a) evaluate the ability of barometric pressure fluctuations on Mars to drive methane transport from depths capable of supporting living microbes (200 m), (b) generate surface flux patterns mirroring the observed seasonality of atmospheric methane abundance, and (c) test the sensitivity of surface methane fluxes to subsurface properties (Table 1). Flow and transport equations in the fractures are coupled to transport equations in the rock matrix to simulate the overall behavior of gases in fractured rock. These approaches are standard in subsurface hydrogeology—the governing equations and computational approach are described in detail in Section 3 in Supporting Information S1. Calculations are performed within the Finite-Element Heat and Mass (FEHM) simulator, a well-tested multiphase code (Zyvoloski et al., 1999, 2017, 2021). FEHM has been used extensively in terrestrial barometric pumping studies (Bourret et al., 2019, 2020; Jordan et al., 2014, 2015; Neeper & Stauffer, 2012a, 2012b; Stauffer et al., 2019). We have made a simplifying assumption that there is no water in the domain, which would reduce available air-filled porosity (as ice) and cause temporary immobile storage due to phase partitioning (as liquid). Gravity and air properties are modified for this study to replicate Mars conditions.

2.1. Boundary Conditions

The simulations are run under isothermal conditions using Mars air (~95% CO₂) and methane properties consistent with the mean surface temperature at Gale crater (−50°C). The bottom of the domain is a no-flux boundary, representing an impermeable bedrock or ice layer at depth. The left and right lateral boundaries are no-flux boundaries. The top boundary is forced by the barometric pressure record collected by the *Curiosity* Mars Science Laboratory Rover Environmental Monitoring Station (MSL-REMS; <https://pds.nasa.gov/>).

Vapor-phase methane and martian air are allowed to escape the domain from the top boundary. We prescribed a continuous methane production rate ($9.6 \times 10^{-7} \text{ mg CH}_4 \text{ m}^{-3} \text{ sol}^{-1}$) within a 5-m-thick zone at the bottom spanning the lateral extent of the domain (Figure 2). This rate is consistent with measurements of methanogenic microbes at depth in Mars-analog terrestrial settings (Colwell et al., 2008; Onstott et al., 2006). Coincidentally, this rate is of the same order of magnitude as liberal estimates of the maximum methane

Table 1
Geologic Properties of the Subsurface Model

Case	ϕ_m [–]	k_m [m ²]	k_f [m ²]
Base case	0.35	1×10^{-14}	8.3×10^{-10}
High k_m	0.35	1×10^{-12}	8.3×10^{-10}
Low k_m	0.35	1×10^{-17}	8.3×10^{-10}
Low ϕ_m	0.10	1×10^{-14}	8.3×10^{-10}
Narrow b	0.35	1×10^{-14}	8.3×10^{-12}

Note. ϕ_m is the matrix porosity (unitless), and k_m and k_f are the matrix and fracture permeability (m²), respectively. Fracture porosity ϕ_f is assumed 1.0. The fracture permeability k_f in the table is upscaled in the model to the numerical mesh dimensions following the procedure described in Section 4.2 in Supporting Information S1.

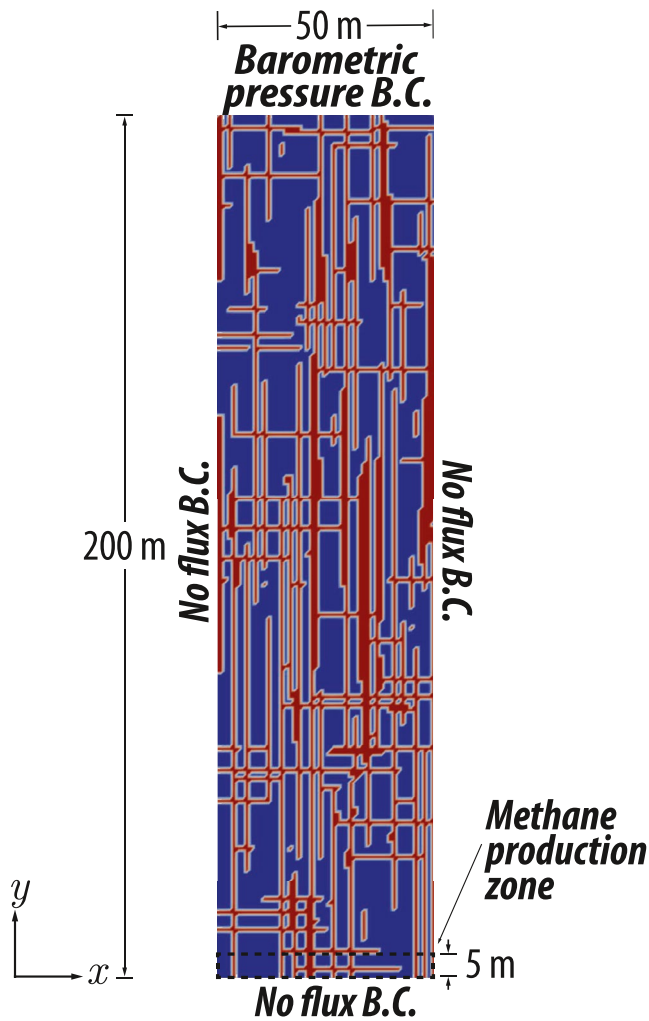


Figure 2. Vertical cross-section of the fracture network generated using the Lévy-Lee algorithm. Fractures are shown in red, with rock matrix in blue (B.C. = boundary condition). A methane source located in the methane production zone produces methane at a rate of $6.7 \times 10^{-16} \text{ mol CH}_4 \text{ m}^{-3} \text{ s}^{-1}$.

production rate by serpentinization reactions on Mars (Stevens et al., 2015). Our model thus assumes direct source rock to seepage pathway similar to that observed in Etiope et al. (2013), rather than a source-reservoir-seepage system.

Before beginning the transport simulation, we initialize the flow model using a constant surface pressure for 10^8 years to create an air-static equilibrium gradient throughout the subsurface. We used this air-static equilibrium as the initial state for the transport simulations. The MSL pressure record (2,713 sols long at the time of simulation) is extended by cyclically repeating the record to provide the surface pressure boundary condition. Transport simulations are run for 60,000 sols, by which point the system in each case has reached a cyclical quasi-steady-state, as determined by a linear trend in cumulative surface mass outflow. The domain is initially populated with a uniform concentration of methane gas ($C_0 = 9.6 \times 10^{-5} \text{ mol kg}_{\text{air}}^{-1}$) to allow the subsurface to more efficiently reach a quasi-equilibrium by pumping out excess methane from the system in the early stages of the simulation. After we achieve cyclical quasi-steady-state transport conditions, we can calculate the time-averaged surface flux for key periods (e.g., the large peak in northern summer and small peak in northern winter).

2.2. Geologic Framework

We assigned the background rock matrix in the base case a porosity (ϕ_m) of 35%, which is in the range estimated by Lewis et al. (2019) based on consideration of the low bedrock density at Gale crater. We set the background rock permeability (k_m) to $1 \times 10^{-14} \text{ m}^2$ (0.01 Darcies). This is slightly more permeable than the conservative $3 \times 10^{-15} \text{ m}^2$ prescribed by previous research modeling hydrothermal circulation on Mars (Lyons et al., 2005), which is appropriate as our domain is much shallower than the domain considered there ($\sim 10 \text{ km}$), and permeability tends to decrease with depth (Manning & Ingebritsen, 1999). We assumed a fracture porosity (ϕ_f) of 100% (i.e., open fractures); we calculated fracture permeability (k_f) as $k_f = b^2/12 = 8.3 \times 10^{-10} \text{ m}^2$ assuming a fracture aperture (b) of 0.1 mm for all fractures in the domain. Rock properties are presented in Table 1. Other scenarios with the same fracture network topology (described below in Section 2.3) were tested by varying the rock matrix properties (Table 1). We also ran several alternative simulations to the base case, including: simulations with shallower methane source depths (150 and 50 m), a simulation

having narrower fractures (aperture $b = 0.01 \text{ mm}$) and wider fractures ($b = 1 \text{ mm}$), as well as cases with, respectively, a much higher methane production rate ($6.7 \times 10^{-12} \text{ mol CH}_4 \text{ m}^{-3} \text{ s}^{-1}$) in the source zone and depth-dependent fracture density.

2.3. Numerical Mesh

We set up the model in FEHM as a two-dimensional planar domain 50 m wide by 200 m deep. Mesh discretization is uniform in the x and y directions such that $\Delta x = \Delta y = 1 \text{ m}$. We randomly generated orthogonal discrete fractures using the 2-D Lévy-Lee algorithm (Clemons & Smith, 1997), a fractal-based fracture model first presented in Geier et al. (1988) and described in detail in Section 4.1 in Supporting Information S1. The Lévy-Lee algorithm generates a fracture network with a continuum of scales for both fracture length and spacing between fractures (Figure 2). The Lévy-Lee algorithm is found to accurately describe fracture networks in a range of geological and tectonic settings. Although the model can be constructed with non-orthogonal and inclined fractures, the overall behavior is dominated by the connectivity among highly permeable fractures rather than their orientation; for this reason, we employed a relatively simple domain with orthogonal fractures. We then mapped the fracture network onto a uniform grid, which essentially embeds the fractures in the rock matrix via upscaling

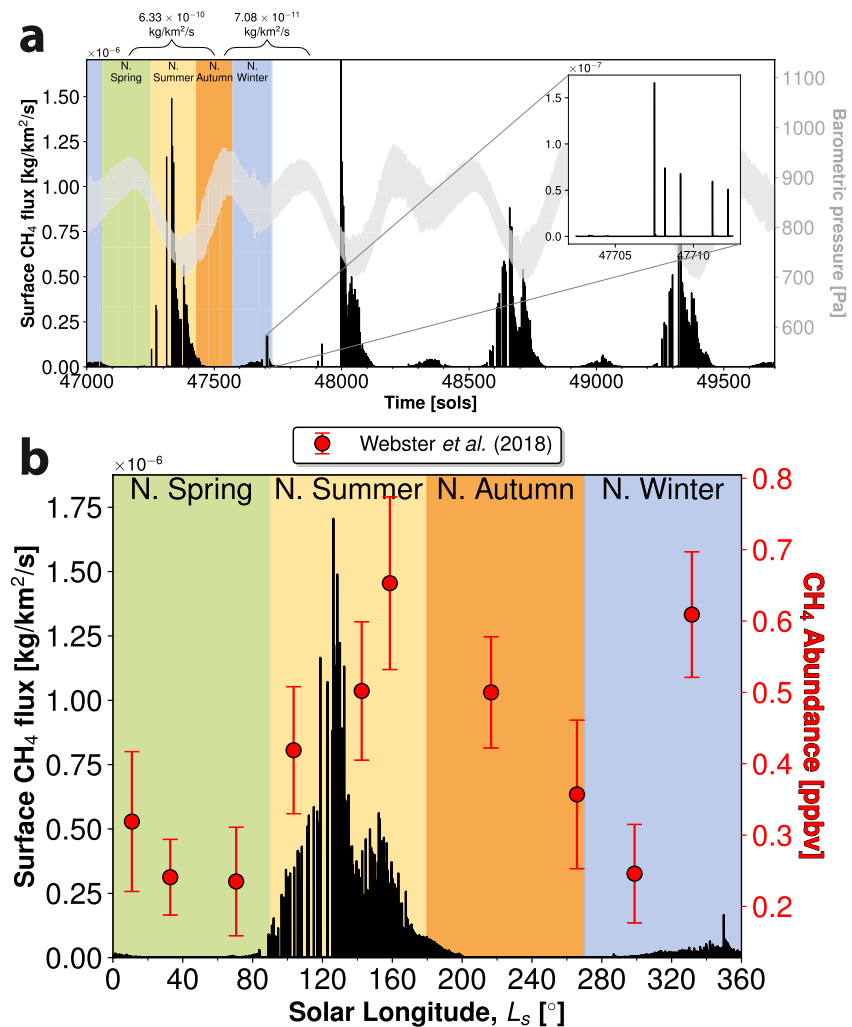


Figure 3. (a) Base case surface methane flux (black), with barometric pressure (gray) driving the subsurface transport model. Pressure records were collected by Mars Science Laboratory (MSL) and are repeated in the simulations cyclically. The plot shows the surface fluxes for a 2,713-sol period when the model had reached a cyclical pseudo-steady state. Annotations with curly braces indicate time averaged fluxes for the 334-sol spans shown, each centered on the local flux maximum within that period. Colored zones indicate Mars seasons for the northern hemisphere. Inset figure highlights the diurnal and semi-diurnal variations in surface flux. (b) Base case simulated surface methane flux (black) plotted against solar longitude (L_s) compared to atmospheric methane abundances at Gale crater (red circles), which were collected by the *Curiosity* TLS-SAM instrument suite (Webster et al., 2018). Error bars show ± 1 standard error of the mean.

of properties (Section 4.2 in Supporting Information S1), allowing two-way coupling of air and methane fluxes across the fracture-matrix interface.

We generated the fracture network to be somewhat representative of Mars' subsurface (see Section 4.3 in Supporting Information S1). Because the subsurface on Mars is so poorly characterized, we estimate the fracture density (i.e., the ratio of fracture volume to bulk rock volume) based on rover photographs depicting surface expression of fracture networks at Gale crater and extrapolated their distribution into the subsurface. This approximation likely represents an upper limit of fracture density since lithostatic pressures tend to close fractures with depth.

3. Results and Discussion

Our results (Figure 3a, Table 2) illustrate the ability of barometric pumping to induce significant methane transport to the martian atmosphere from considerably deeper sources than prior subsurface transport studies. Recent work by Viúdez-Moreiras et al. (2020) determined using a porous-media model that advective transport would

Table 2
Time-Averaged Fluxes for Different Time Windows Centered on the Large Northern Summer High-Methane Period and Smaller Northern Winter High-Methane Period

Case	Time-averaged flux 10^{-9} [kg·km ⁻² ·s ⁻¹]						Figures
	Northern summer			Northern winter			
	Window duration [sols]			Window duration [sols]			
	58	117	334	58	117	334	
Base case	1.80	1.30	0.63	0.17	0.16	0.07	3a
High matrix permeability (k_m)	3.02	2.66	1.39	0.66	0.54	0.29	S10
Low matrix permeability (k_m)	0.83	0.74	0.41	0.12	0.11	0.06	S11
Low matrix porosity (ϕ_m)	0.05	0.04	0.02	0.006	0.005	0.002	S12
Shallow source (50 m)	5.02	3.71	1.84	0.47	0.43	0.18	S13
Shallow source (150 m)	1.83	1.32	0.64	0.18	0.17	0.07	S14
Narrow fractures ($b = 0.01$ mm)	0.24	0.18	0.07	0.001	0.0009	0.0004	S15
Wide fractures ($b = 1$ mm)	413.0	364.8	188.2	85.81	61.96	30.31	S16
High CH ₄ production rate	890.2	644.7	314.1	84.82	79.58	34.52	S17
Depth-depend. fract. density	1.99	1.44	0.69	0.19	0.18	0.08	S18
Moores, Gough et al. (2019)			8.40 ^a				
Moores, King, et al. (2019)			1.69 ^b				
Moores, King, et al. (2019)			1.13 ^c			0.43 ^c	
Moores, King, et al. (2019)			2.83 ^d			0.78 ^d	
Formisano et al. (2004)			0.028 ^e				

^aUpper limit assuming seepage restricted to Gale crater. ^bAverage accounting for diurnal atmospheric mixing variations. ^cAnnual maximum/minimum for a completely stably stratified atmospheric model. ^dAnnual maximum/minimum for a well-mixed near-surface atmospheric model. ^eAssuming continuous, uniform planet-wide seepage.

be limited to the first few meters of depth. In contrast, atmospheric pressure fluctuations can produce significant advective flow at great depths within a network of connected fractures. Our model provides a physical representation of the upward ratcheting mechanism described above, and it explicitly represents both a fracture network and rock matrix blocks with highly contrasting permeabilities. With this geologic framework, the barometric pumping mechanism is able to produce significant surface seepage from depths of 200 m (Figures 3a and 3b), which is our estimated likely minimum depth of potentially living methanogenic microbes (Section 1 in Supporting Information S1).

Our simulations reveal strong periodicity associated with methane seepage driven by seasonal barometric pressure fluctuations on Mars (Figures 3a and 3b), which closely resembles the intermittent seepage pattern described for terrestrial emissions in Etiope and Oehler (2019, Figure 1b). In our results, the highest-intensity methane spikes occur in northern summer/southern winter (solar longitude, L_s , 90–180°; Gale crater at 5.4°S, 137.4°E is near the equator). This pattern is consistent with recent work that found strong seasonal cycles of background methane levels at Gale crater (Figure 3b) based on measurements of atmospheric methane abundance collected by the *Curiosity* Tunable Laser Spectrometer (TLS) of the Sample Analysis at Mars (SAM) instrument suite (Webster et al., 2018). Additionally, Webster et al. (2018) observed a weak correlation between lower maximum pressure-per-sol and higher methane concentrations (Webster et al., 2018), which may also be explained by the barometric-pumping mechanism. We found a linear correlation (Pearson correlation coefficient = 0.62; Figure S9 in Supporting Information S1) between simulated surface flux and the atmospheric methane abundance measurements from *Curiosity* (Webster et al., 2018), which we discuss in Section 5.2 in Supporting Information S1. This relationship is expected because increased surface methane flux will increase levels of atmospheric methane under simple mixing conditions, although wind, atmospheric mixing rates, planetary boundary layer height, photochemical destruction, and other factors lead to deviations from strict proportionality.

In our base case simulation (Figure 3a), we calculate time-averaged fluxes for two characteristic high-methane periods—each spanning 334 sols (0.5 martian years, and nearly 1 Earth year). In a given Mars year (668 sols, L_s 0–360°), the barometric pumping mechanism driven by martian atmospheric pressures produces one large peak of methane flux (time-averaged flux of order $6 \times 10^{-10} \text{ kg km}^{-2} \text{ s}^{-1}$) occurring in northern summer, and one small peak of methane flux (of order $7 \times 10^{-11} \text{ kg km}^{-2} \text{ s}^{-1}$) occurring in northern winter. Maximum diurnal methane spikes can be several orders of magnitude greater ($\sim 0.2\text{--}1.8 \times 10^{-6} \text{ kg km}^{-2} \text{ s}^{-1}$; Figure 3a). Both the large and small methane flux peaks coincide with the troughs of downward-trending atmospheric pressures, which makes sense intuitively, as these conditions create a favorable subsurface pressure gradient for promoting upward advective transport. We present time-averaged fluxes for all simulations in Table 2, with multiple time window durations for interpreting shorter-term seepage events.

Methane fluxes calculated in our simulations are comparable to the range of previous flux estimates based on observed atmospheric methane abundances on Mars (Table 2; Figures 3a, S10, S11, S12 in Supporting Information S1). Estimates of methane surface flux on Mars range from $2 \times 10^{-11} \text{ kg km}^{-2} \text{ s}^{-1}$ (assuming planet-wide, uniform seepage; Formisano et al., 2004) to $8.4 \times 10^{-9} \text{ kg km}^{-2} \text{ s}^{-1}$, which is based on an upper-limit estimate of methane microseepage at Gale crater (Moores, Gough et al., 2019). The most current estimate of surface fluxes at Gale crater is provided by constraining a microseepage-fed adsorptive-diffusive process with SAM-TLS and ExoMars Trace Gas Orbiter measurements (Moores, King et al., 2019). By also taking into account diurnal atmospheric mixing variations, the surface methane flux at Gale crater was determined to be $1.5 \times 10^{-10} \text{ kg m}^{-2} \text{ sol}^{-1}$ ($1.69 \times 10^{-9} \text{ kg km}^{-2} \text{ s}^{-1}$), which would require an emission area of $2.7 \times 10^4 \text{ km}^2$ (approximately 143% of the area of Gale crater itself) to supply the annual planet-wide atmospheric methane budget ($\sim 4.0 \text{ kg/sol}$, or about 2.7 tonnes per martian year) (Korablev et al., 2019). Depending on the atmospheric model end-members used in that study (Table 2, superscripts b–d), flux was found to vary over the martian year by a factor of 3.0–3.6 (Moores, King et al., 2019). In comparison, average surface flux for our base case simulation over the course of one martian year (668 sols) is approximately $3 \times 10^{-10} \text{ kg km}^{-2} \text{ s}^{-1}$, which would require emissions from approximately $1.3 \times 10^5 \text{ km}^2$ (~ 8 times the area of Gale crater, or $\sim 0.1\%$ the total surface area of Mars) to supply the planet-wide methane budget. Base case flux varies over a martian year by a factor of 9 when comparing the large and small high-methane periods of our base case simulation. The actual magnitude of flux is controlled by a number of factors. For example, greater source strength (Figure S17 in Supporting Information S1), shallower source depth (Figure S13 in Supporting Information S1), or elevated subsurface pressures caused by geologic stresses would all promote greater methane fluxes. Conversely, deeper source depth or narrower fracture apertures (Figure S15 in Supporting Information S1) would result in reduced methane fluxes.

We performed an analogous base case simulation for a source depth of 50 m (Figure S13 in Supporting Information S1) which exhibited roughly three times the time-averaged flux compared to the base case. Better understanding of source terms and characterization of Mars' subsurface would greatly improve such calculations. Furthermore, transport is likely affected by additional physico-chemical processes, such as adsorption (Moores, Gough, et al., 2019; Moores, King et al., 2019) to mineral grains in the shallow regolith, which would also affect the magnitude and timing of surface release of methane.

4. Conclusions

We have proposed that barometric pumping in a fractured subsurface provides a mechanism for venting methane from deep sources to the atmosphere on Mars. Our flow and transport simulations in fractured rock demonstrate that barometric pumping is capable of producing significant surface fluxes of methane (Figure 3a), even when the methane source is at considerable depth (200 m). A key factor is the relatively high fracture density in the lower gravity environment of Mars (Lewis et al., 2019). Our simulations confirm the clear connection between atmospheric pressures and surface methane flux (Figures 3a and 3b; S9 in Supporting Information S1) hypothesized in previous works (Etiope & Oehler, 2019). Driven by atmospheric pressure fluctuations acquired by the *Curiosity* REMS barometric record, the overall surface seepage pattern at Gale crater is highly seasonal, with local flux maxima generally occurring during times of low atmospheric pressure. It is noteworthy that the seasonality of fluxes generated in our model (Figure 3b) is reasonably consistent (Figure S9 in Supporting Information S1) with that of atmospheric methane abundance variations found in previous research (Webster et al., 2018). The overall magnitude of fluxes in our model (Table 2) is within the range of previously reported values for surface methane seepage (Formisano et al., 2004; Moores, Gough, et al., 2019; Moores, King et al., 2019; Mumma et al., 2009).

Relatively large average flux during high-methane periods in our simulations supports a conceptual model of short-duration, localized surface releases rather than a homogeneous (planet-wide), constant release of methane (Table 2).

To our knowledge, this analysis is the first to make an explicit mechanistic connection between deep subsurface methane stores and the observed seasonality of atmospheric methane concentrations on Mars. Emission mechanisms proposed to date (Yung et al., 2018) have had difficulties explaining the methane abundance variations detected by MSL (Webster et al., 2018; Yung et al., 2018), although one study was largely able to match methane abundance seasonality with a model of methane transport by diffusion and adsorption from a relatively shallow (<30 m) source (Moores, Gough, et al., 2019). We have demonstrated that barometric pumping transport in a fractured subsurface can reconcile the methane abundance variations detected by MSL with emissions from subsurface reservoirs by regulating emissions via meteorological conditions, rather than requiring a time-varying methane production or release mechanism to explain the observed episodicity. Until now, the inability to identify and study a mechanism for significant, rapid transport of methane from depths >10–30 m on Mars has led to conclusions that periodic rapid spikes in atmospheric methane can only be tied to transport from very shallow accumulations (Chastain & Chevrier, 2007; Hu et al., 2016; Max et al., 2013; Moores, Gough, et al., 2019; Moores, King et al., 2019), which implicitly ruled out living microbial methanogens as a source of methane on Mars (Section 1 in Supporting Information S1). Our results confirm the viability of rapid, efficient periodic methane transport from depths that are hospitable to potentially living microbial methanogens, supporting the possibility that Mars methane may be produced by extant microorganisms.

Data Availability Statement

Pressure data described in the paper are further described in the supplementary materials and were acquired from NASA's Planetary Data System (PDS) at the following address: https://atmos.nmsu.edu/PDS/data/mslrem_1001/DATA/. PDS data products from the Mars Science Laboratory (MSL) Rover Environmental Monitoring Station (REMS) were used for the analysis in this paper. The MSL REMS Models Reduced Data Record (MODRDR) provided the atmospheric pressure measurements for our simulations (Gómez-Elvira, 2019a). The MSL REMS Ancillary Data Record (ADR) provided the rover elevations we used in our elevation corrections to pressure measurements (Gómez-Elvira, 2019b). Figures were made with Matplotlib version 3.2.2 (Hunter, 2007) available under the Matplotlib license at <https://matplotlib.org/>. The FEHM software (Zyvoloski, 2007; Zyvoloski et al., 2017) version 3.4.0 (<https://fehm.lanl.gov>) associated with this manuscript for the simulation of gas flow and transport is published on GitHub: <https://github.com/lanl/FEHM/tree/v3.4.0>.

Acknowledgments

This research was supported by the Los Alamos National Laboratory (LANL) through its Center for Space and Earth Science (CSES). J. P. Ortiz, P. H. Stauffer, D. R. Harp, and R. C. Wiens are (or were) employed by LANL at the time of writing, and J. P. Ortiz, P. H. Stauffer, and D. R. Harp were funded by the CSES grant. CSES is funded by LANL's Laboratory Directed Research and Development (LDRD) program under project number 20210528CR. Los Alamos National Laboratory is operated by Triad National Security, LLC, for the National Nuclear Security Administration of U.S. Department of Energy (Contract No. 89233218CNA000001). LA-UR-22-20869. The review comments of two anonymous reviewers are gratefully acknowledged.

References

- Auer, L. H., Rosenberg, N. D., Birdsell, K. H., & Whitney, E. M. (1996). The effects of barometric pumping on contaminant transport. *Journal of Contaminant Hydrology*, 24(2), 145–166.
- Bourret, S. M., Kwicklis, E. M., Harp, D. R., Ortiz, J. P., & Stauffer, P. H. (2020). Beyond Barnwell: Applying lessons learned from the Barnwell site to other historic underground nuclear tests at Pahute Mesa to understand radioactive gas-seepage observations. *Journal of Environmental Radioactivity*, 222, 1–14. <https://doi.org/10.1016/j.jenvrad.2020.106297>
- Bourret, S. M., Kwicklis, E. M., Miller, T. A., & Stauffer, P. H. (2019). Evaluating the importance of barometric pumping for subsurface gas transport near an underground nuclear test site. *Vadose Zone Journal*, 18(1), 1–17. <https://doi.org/10.2136/vzj2018.07.0134>
- Buckingham, E. (1904). *Contributions to our knowledge of the aeration of soils* (Vol. 25; Tech. Rep.). US Department of Agriculture.
- Carrigan, C. R., Heinle, R. A., Hudson, G. B., Nitao, J. J., & Zucca, J. J. (1996). Trace gas emissions on geological faults as indicators of underground nuclear testing. *Nature*, 382(6591), 528–531. <https://doi.org/10.1038/382528a0>
- Carrigan, C. R., Heinle, R. A., Hudson, G. B., Nitao, J. J., & Zucca, J. J. (1997). *Barometric gas transport along faults and its application to nuclear test-ban monitoring* (Tech. Rep. No. May). Lawrence Radiation Laboratory.
- Carroll, S. A., Keating, E., Mansoor, K., Dai, Z., Sun, Y., Trainor-Guitton, W., et al. (2014). Key factors for determining groundwater impacts due to leakage from geologic carbon sequestration reservoirs. *International Journal of Greenhouse Gas Control*, 29, 153–168.
- Chastain, B. K., & Chevrier, V. (2007). Methane clathrate hydrates as a potential source for martian atmospheric methane. *Planetary and Space Science*, 55(10), 1246–1256. <https://doi.org/10.1016/j.pss.2007.02.003>
- Clemo, T. M., & Smith, L. (1997). A hierarchical model for solute transport in fractured media. *Water Resources Research*, 33(8), 1763–1783.
- Colwell, F. S., Boyd, S., Delwiche, M. E., Reed, D. W., Phelps, T. J., & Newby, D. T. (2008). Estimates of biogenic methane production rates in deep marine sediments at Hydrate Ridge, Cascadia margin. *Applied and Environmental Microbiology*, 74(11), 3444–3452. <https://doi.org/10.1128/AEM.02114-07>
- De Toffoli, B., Pozzobon, R., Mazzarini, F., Orgel, C., Massironi, M., Giacomini, L., et al. (2018). Estimate of depths of source fluids related to mound fields on Mars. *Planetary and Space Science*, 164, 164–173.
- Dempsey, D., Kelkar, S., & Pawar, R. (2014). Passive injection: A strategy for mitigating reservoir pressurization, induced seismicity and brine migration in geologic CO₂ storage. *International Journal of Greenhouse Gas Control*, 28, 96–113.

- Etiopio, G., Drobnik, A., & Schimmelmann, A. (2013). Natural seepage of shale gas and the origin of “eternal flames” in the Northern Appalachian Basin, USA. *Marine and Petroleum Geology*, *43*, 178–186. <https://doi.org/10.1016/j.marpetgeo.2013.02.009>
- Etiopio, G., & Martinelli, G. (2002). Migration of carrier and trace gases in the geosphere: An overview. *Physics of the Earth and Planetary Interiors*, *129*(3–4), 185–204. [https://doi.org/10.1016/S0031-9201\(01\)00292-8](https://doi.org/10.1016/S0031-9201(01)00292-8)
- Etiopio, G., & Oehler, D. Z. (2019). Methane spikes, background seasonality and non-detections on Mars: A geological perspective. *Planetary and Space Science*, *168*(February), 52–61. <https://doi.org/10.1016/j.pss.2019.02.001>
- Formisano, V., Atreya, S. K., Encrenaz, T., Ignatiev, N., & Giuranna, M. (2004). Detection of methane in the atmosphere of Mars. *Science*, *306*(5702), 1758–1761.
- Geier, J. E., Lee, K., & Dershowitz, W. S. (1988). Field validation of conceptual models for fracture geometry. *Transactions – American Geophysical Union*, *69*(44), 1177.
- Giuranna, M., Viscardi, S., Daerden, F., Neary, L., Etiopio, G., Oehler, D., et al. (2019). Independent confirmation of a methane spike on Mars and a source region east of Gale Crater. *Nature Geoscience*, *12*(5), 326–335. <https://doi.org/10.1038/s41561-019-0331-9>
- Gómez-Elvira, J. (2019a). MSL Mars Rover Environmental Monitoring Station Models Data Archive V1.0. [Dataset]. MSL. <https://doi.org/10.17189/GHBC-QR41>
- Gómez-Elvira, J. (2019b). MSL Mars Rover Environment Monitoring Station Ancillary Data V1.0. [Dataset]. MSL. <https://doi.org/10.17189/YJDT-2F87>
- Harp, D. R., Bourret, S. M., Stauffer, P. H., & Kwicklis, E. M. (2020). Discriminating underground nuclear explosions leading to late-time radionuclide gas seeps. *Geophysical Research Letters*, *47*(13), 1–8. <https://doi.org/10.1029/2019GL086654>
- Harp, D. R., Ortiz, J. P., Pandey, S., Karra, S., Anderson, D. N., Bradley, C. R., et al. (2018). Immobile pore-water storage enhancement and retardation of gas transport in fractured rock. *Transport in Porous Media*, *124*, 369–394. <https://doi.org/10.1007/s11242-018-1072-8>
- Heap, M. J., Byrne, P. K., & Mikhail, S. (2017). Low surface gravitational acceleration of Mars results in a thick and weak lithosphere: Implications for topography, volcanism, and hydrology. *Icarus*, *281*, 103–114. <https://doi.org/10.1016/j.icarus.2016.09.003>
- Hu, R., Bloom, A. A., Gao, P., Miller, C. E., & Yung, Y. L. (2016). Hypotheses for near-surface exchange of methane on Mars. *Astrobiology*, *16*(7), 539–550. <https://doi.org/10.1089/ast.2015.1410>
- Hunter, J. D. (2007). Matplotlib: A 2D graphics environment [Software]. *Computing in Science & Engineering*, *9*(3), 90–95. <https://doi.org/10.5281/zenodo.3898017>
- Jordan, A. B., Stauffer, P. H., Knight, E. E., Rougier, E., & Anderson, D. N. (2015). Radionuclide gas transport through nuclear explosion-generated fracture networks. *Nature Scientific Reports*, *5*(December), 1–10. <https://doi.org/10.1038/srep18383>
- Jordan, A. B., Stauffer, P. H., Zvoloski, G. A., Person, M. A., MacCarthy, J. K., & Anderson, D. N. (2014). Uncertainty in prediction of radionuclide gas migration from underground nuclear explosions. *Vadose Zone Journal*, *13*(10), 1–13. <https://doi.org/10.2136/vzj2014.06.0070>
- Knapmeyer-Endrun, B., Panning, M. P., Bissig, F., Joshi, R., Khan, A., Kim, D., et al. (2021). Thickness and structure of the martian crust from InSight seismic data. *Science*, *373*(6553), 438–443. <https://doi.org/10.1126/science.abf8966>
- Korablev, O., Vandaele, A. C., Montmessin, F., Fedorova, A. A., Trokhimovskiy, A., Forget, F., et al. (2019). No detection of methane on Mars from early ExoMars Trace Gas Orbiter observations. *Nature*, *568*(7753), 517–520. <https://doi.org/10.1038/s41586-019-1096-4>
- Krasnopolsky, V. A., Maillard, J. P., & Owen, T. C. (2004). Detection of methane in the martian atmosphere: Evidence for life? *Icarus*, *172*(2), 537–547. <https://doi.org/10.1016/j.icarus.2004.07.004>
- Kronyak, R. E., Kah, L. C., Edgett, K. S., Van Bommel, S. J., Thompson, L. M., Wiens, R. C., et al. (2019). Mineral-filled fractures as indicators of multigenerational fluid flow in the Pahrump Hills member of the Murray formation, Gale crater, Mars. *Earth and Space Science*, *6*(2), 238–265. <https://doi.org/10.1029/2018EA000482>
- Lefèvre, F., & Forget, F. (2009). Observed variations of methane on Mars unexplained by known atmospheric chemistry and physics. *Nature*, *460*(7256), 720–723. <https://doi.org/10.1038/nature08228>
- Lewis, K. W., Peters, S., Gonter, K., Morrison, S., Schmerr, N., Vasavada, A. R., & Gabriel, T. (2019). A surface gravity traverse on Mars indicates low bedrock density at Gale crater. *Science*, *363*(6426), 535–537. <https://doi.org/10.1126/science.aat0738>
- Lognonné, P., Banerdt, W. B., Pike, W. T., Giardini, D., Christensen, U., García, R. F., et al. (2020). Constraints on the shallow elastic and anelastic structure of Mars from InSight seismic data. *Nature Geoscience*, *13*(3), 213–220. <https://doi.org/10.1038/s41561-020-0536-y>
- Lyons, J. R., Manning, C. E., & Nimmo, F. (2005). Formation of methane on Mars by fluid-rock interaction in the crust. *Geophysical Research Letters*, *32*(13), 1–4. <https://doi.org/10.1029/2004GL022161>
- Manning, C. E., & Ingebritsen, S. E. (1999). Permeability of the continental crust: Implications of geothermal data and metamorphic systems. *Reviews of Geophysics*, *37*(1), 127–150.
- Massmann, J., & Farrier, D. F. (1992). Effects of atmospheric pressures on gas transport in the vadose zone. *Water Resources Research*, *28*(3), 777–791. <https://doi.org/10.1029/91WR02766>
- Max, M. D., Johnson, A. H., & Clifford, S. M. (2013). Hydrocarbon system analysis for methane hydrate exploration on Mars. *AAPG Memoir*, *101*, 99–114. <https://doi.org/10.1306/13361573M1013546>
- Moore, J. E., Gough, R. V., Martínez, G. M., Meslin, P. Y., Smith, C. L., Atreya, S. K., et al. (2019). Methane seasonal cycle at Gale Crater on Mars consistent with regolith adsorption and diffusion. *Nature Geoscience*, *12*(5), 321–325. <https://doi.org/10.1038/s41561-019-0313-y>
- Moore, J. E., King, P. L., Smith, C. L., Martínez, G. M., Newman, C. E., Guzewich, S. D., et al. (2019). The methane diurnal variation and microseepage flux at Gale crater, Mars as constrained by the ExoMars Trace Gas Orbiter and Curiosity observations. *Geophysical Research Letters*, *46*(16), 9430–9438. <https://doi.org/10.1029/2019GL083800>
- Mumma, M. J., Villanueva, G. L., Novak, R. E., Hewagama, T., Bonev, B. P., DiSanti, M. A., et al. (2009). Strong release of methane on Mars in northern summer 2003. *Science*, *323*(5917), 1041–1045. <https://doi.org/10.1126/science.1165243>
- Myers, T. (2012). Potential contaminant pathways from hydraulically fractured shale to aquifers. *Groundwater*, *50*(6), 872–882.
- Neeper, D. A. (2002). Investigation of the vadose zone using barometric pressure cycles. *Journal of Contaminant Hydrology*, *54*, 59–80.
- Neeper, D. A. (2003). Harmonic analysis of flow in open boreholes due to barometric pressure cycles. *Journal of Contaminant Hydrology*, *60*, 135–162. [https://doi.org/10.1016/S0169-7722\(02\)00086-4](https://doi.org/10.1016/S0169-7722(02)00086-4)
- Neeper, D. A., & Stauffer, P. H. (2012a). Transport by oscillatory flow in soils with rate-limited mass transfer: 1. Theory. *Vadose Zone Journal*, *11*(2), 1–14. <https://doi.org/10.2136/vzj2011.0093>
- Neeper, D. A., & Stauffer, P. H. (2012b). Transport by oscillatory flow in soils with rate-limited mass transfer: 2. Field experiment. *Vadose Zone Journal*, *11*(2), 1–12. <https://doi.org/10.2136/vzj2011.0093>
- Nilson, R. H., Peterson, E. W., Lie, K. H., Burkhard, N. R., & Hearst, J. R. (1991). Atmospheric pumping: A mechanism causing vertical transport of contaminated gases through fractured permeable media. *Journal of Geophysical Research*, *96*(B13), 933–948. <https://doi.org/10.2752/147597509112541>

- Oehler, D. Z., & Etiope, G. (2017). Methane seepage on Mars: Where to look and why. *Astrobiology*, *17*(12), 1233–1264. <https://doi.org/10.1089/ast.2017.1657>
- Onstott, T. C., McGown, D., Kessler, J., Lollar, B. S., Lehmann, K. K., & Clifford, S. M. (2006). Martian CH₄: Sources, flux, and detection. *Astrobiology*, *6*(2), 377–395.
- Pan, L., Oldenburg, C. M., Pruess, K., & Wu, Y.-S. (2011). Transient CO₂ leakage and injection in wellbore-reservoir systems for geologic carbon sequestration. *Greenhouse Gases: Science and Technology*, *1*(4), 335–350.
- Rey, A., Belelli-Marchesini, L., Etiope, G., Papale, D., Canfora, E., Valentini, R., & Pegoraro, E. (2014). Partitioning the net ecosystem carbon balance of a semiarid steppe into biological and geological components. *Biogeochemistry*, *118*(1–3), 83–101. <https://doi.org/10.1007/s10533-013-9907-4>
- Rodríguez, J. A. P., Sasaki, S., Dohm, J. M., Tanaka, K. L., Strom, B., Kargel, J., et al. (2005). Control of impact crater fracture systems on subsurface hydrology, ground subsidence, and collapse, Mars. *Journal of Geophysical Research: Planets*, *110*(6), 1–22. <https://doi.org/10.1029/2004JE002365>
- Roos-Serote, M., Atreya, S. K., Webster, C. R., & Mahaffy, P. R. (2016). Cometary origin of atmospheric methane variations on Mars unlikely. *Journal of Geophysical Research: Planets*, *121*(10), 2108–2119. <https://doi.org/10.1002/2016JE005076>
- Stauffer, P. H., Rahn, T. A., Ortiz, J. P., Joseph, S. L., Boukhalfa, H., & Snyder, E. E. (2018). *Summary of a gas transport tracer test in the Deep Cerros Del Rio Basalts, Mesita del Buey, Los Alamos NM (Tech. Rep.)*. Los Alamos National Laboratory.
- Stauffer, P. H., Rahn, T. A., Ortiz, J. P., Salazar, L. J., Boukhalfa, H., Behar, H. R., & Snyder, E. E. (2019). Evidence for high rates of gas transport in the deep subsurface. *Geophysical Research Letters*, *46*, 3773–3780. <https://doi.org/10.1029/2019GL082394>
- Stevens, A. H., Patel, M. R., & Lewis, S. R. (2015). Numerical modelling of the transport of trace gases including methane in the subsurface of Mars. *Icarus*, *250*, 587–594.
- Stevens, A. H., Patel, M. R., & Lewis, S. R. (2017). Modelled isotopic fractionation and transient diffusive release of methane from potential subsurface sources on Mars. *Icarus*, *281*, 240–247.
- Sun, Y., & Carrigan, C. R. (2014). Modeling noble gas transport and detection for the Comprehensive Nuclear-Test-Ban Treaty. *Pure and Applied Geophysics*, *171*, 735–750. <https://doi.org/10.1007/s00024-012-0514-4>
- Takle, E. S., Massman, W. J., Brandle, J. R., Schmidt, R. A., Zhou, X., Litvina, I. V., et al. (2004). Influence of high-frequency ambient pressure pumping on carbon dioxide efflux from soil. *Agricultural and Forest Meteorology*, *124*(3–4), 193–206. <https://doi.org/10.1016/j.agrformet.2004.01.014>
- Temel, O., Karatekin, Ö., Gloesener, E., Mischna, M. A., & van Beeck, J. (2019). Atmospheric transport of subsurface, sporadic, time-varying methane releases on Mars. *Icarus*, *325*(2017), 39–54. <https://doi.org/10.1016/j.icarus.2019.02.014>
- Tsang, Y. W., & Narasimhan, T. N. (1992). Effects of periodic atmospheric pressure variation on radon entry into buildings. *Journal of Geophysical Research*, *97*(B6), 9161–9170.
- Villanueva, G. L., Mumma, M. J., Novak, R. E., Radeva, Y. L., Käufel, H. U., Smette, A., et al. (2013). A sensitive search for organics (CH₄, CH₃OH, H₂CO, C₂H₆, C₂H₂, C₂H₄), hydroperoxyl (HO₂), nitrogen compounds (N₂O, NH₃, HCN) and chlorine species (HCl, CH₃Cl) on Mars using ground-based high-resolution infrared spectroscopy. *Icarus*, *223*(1), 11–27. <https://doi.org/10.1016/j.icarus.2012.11.013>
- Viswanathan, H. S., Pawar, R. J., Stauffer, P. H., Kaszuba, J. P., Carey, J. W., Olsen, S. C., et al. (2008). Development of a hybrid process and system model for the assessment of wellbore leakage at a geologic CO₂ sequestration site. *Environmental Science & Technology*, *42*(19), 7280–7286. <https://doi.org/10.1021/es800417x>
- Viúdez-Moreiras, D., Arvidson, R. E., Gómez-Elvira, J., Webster, C., Newman, C. E., Mahaffy, P., & Vasavada, A. R. (2020). Advective fluxes in the martian regolith as a mechanism driving methane and other trace gas emissions to the atmosphere. *Geophysical Research Letters*, *47*(3), 1–8. <https://doi.org/10.1029/2019GL085694>
- Webster, C. R., Mahaffy, P. R., Atreya, S. K., Flesch, G. J., Mischna, M. A., Meslin, P. Y., et al. (2015). Mars methane detection and variability at Gale crater. *Science*, *347*(6220), 415–417. <https://doi.org/10.1126/science.1261713>
- Webster, C. R., Mahaffy, P. R., Atreya, S. K., Moores, J. E., Flesch, G. J., Malespin, C., et al. (2018). Background levels of methane in Mars' atmosphere show strong seasonal variations. *Science*, *360*(6393), 1093–1096.
- Yung, Y. L., Chen, P., Nealson, K., Atreya, S. K., Beckett, P., Blank, J. G., et al. (2018). Methane on Mars and habitability: Challenges and responses. *Astrobiology*, *18*(10), 1221–1242. <https://doi.org/10.1089/ast.2018.1917>
- Zahnle, K., Freedman, R. S., & Catling, D. C. (2011). Is there methane on Mars? *Icarus*, *212*(2), 493–503. <https://doi.org/10.1016/j.icarus.2010.11.027>
- Zyvoloski, G. A. (2007). *FEHM: A control volume finite element code for simulating subsurface multi-phase multi-fluid heat and mass transfer (Tech. Rep.)*. Los Alamos National Laboratory.
- Zyvoloski, G. A., Robinson, B. A., Dash, Z. V., Chu, S., & Miller, T. A. (2017). FEHM: Finite Element Heat and Mass Transfer Code. [Software]. GitHub. Retrieved from <https://github.com/lanl/FEHM/tree/v3.4.0>
- Zyvoloski, G. A., Robinson, B. A., Dash, Z. V., Kelkar, S., Viswanathan, H. S., Pawar, R. J., et al. (2021). Software users manual (UM) for the FEHM application version 3.1-3X. Los Alamos National Laboratory Report LA-UR. -12-24493.
- Zyvoloski, G. A., Robinson, B. A., Dash, Z. V., & Trease, L. L. (1999). *Models and methods summary for the FEHM application (Tech. Rep.)*. Los Alamos National Laboratory.

References From the Supporting Information

- Adobe Inc. (2019). Adobe Illustrator. [Software]. Adobe. Retrieved from <https://adobe.com/products/illustrator>
- Birdsell, D. T., Rajaram, H., Dempsey, D., & Viswanathan, H. S. (2015). Hydraulic fracturing fluid migration in the subsurface: A review and expanded modeling results. *Water Resources Research*, *51*(9), 7159–7188. <https://doi.org/10.1002/2015WR017810>
- Boston, P. J., Ivanov, M. V., & McKay, C. P. (1992). On the possibility of chemosynthetic ecosystems in subsurface habitats on Mars. *Icarus*, *95*(2), 300–308.
- Carrier, B. L., Beaty, D. W., Meyer, M. A., Blank, J. G., Chou, L., Dassarma, S., et al. (2020). Mars Extant life: What's next? Conference report. *Astrobiology*, *20*(6), 785–814. <https://doi.org/10.1089/ast.2020.2237>
- Chaudhuri, A., Rajaram, H., & Viswanathan, H. (2013). Early-stage hypogene karstification in a mountain hydrologic system: A coupled thermohydrochemical model incorporating buoyant convection. *Water Resources Research*, *49*(9), 5880–5899. <https://doi.org/10.1002/wrcr.20427>
- Cooley, J. W., & Tukey, J. W. (1965). An algorithm for the machine calculation of complex Fourier series. *Mathematics of Computation*, *19*(90), 297–301. <https://doi.org/10.2307/2003354>

- Fu, P., Hao, Y., Walsh, S. D., & Carrigan, C. R. (2016). Thermal drawdown-induced flow channeling in fractured geothermal reservoirs. *Rock Mechanics and Rock Engineering*, 49(3), 1001–1024. <https://doi.org/10.1007/s00603-015-0776-0>
- Fung, L.-K., Hiebert, A. D., & Nghiem, L. X. (1992). Reservoir simulation with a control-volume finite-element method. *SPE Reservoir Engineering*, 7(3), 349–357.
- Haagenson, R., & Rajaram, H. (2021). Seismic diffusivity and the influence of heterogeneity on injection-induced seismicity. *Journal of Geophysical Research: Solid Earth*, 126(6), e2021JB021768. <https://doi.org/10.1029/2021JB021768>
- Jones, E. G., Lineweaver, C. H., & Clarke, J. D. (2011). An extensive phase space for the potential Martian biosphere. *Astrobiology*, 11(10), 1017–1033. <https://doi.org/10.1089/ast.2011.0660>
- Lin, L. H., Hall, J., Onstott, T. C., Gihring, T., Lollar, B. S., Boice, E., et al. (2006). Planktonic microbial communities associated with fracture-derived groundwater in a deep gold mine of South Africa. *Geomicrobiology Journal*, 23(6), 475–497. <https://doi.org/10.1080/01490450600875829>
- Lollar, B. S., Lacrampe-Couloume, G., Slater, G. F., Ward, J., Moser, D. P., Gihring, T. M., et al. (2006). Unravelling abiogenic and biogenic sources of methane in the Earth's deep subsurface. *Chemical Geology*, 226(3–4), 328–339. <https://doi.org/10.1016/j.chemgeo.2005.09.027>
- Mellon, M. T., & Phillips, R. J. (2001). Recent gullies on Mars and the source of liquid water. *Journal of Geophysical Research: Planets*, 106(E10), 23165–23179. <https://doi.org/10.1029/2000JE001424>
- Pandey, S., & Rajaram, H. (2016). Modeling the influence of preferential flow on the spatial variability and time-dependence of mineral weathering rates. *Water Resources Research*, 52(12), 9344–9366. <https://doi.org/10.1111/j.1752-1688.1969.tb04897.x>
- Stamenković, V., Beegle, L. W., Zacny, K., Arumugam, D. D., Baglioni, P., Barba, N., et al. (2019). The next frontier for planetary and human exploration. *Nature Astronomy*, 3(2), 116–120. <https://doi.org/10.1038/s41550-018-0676-9>
- Stamenković, V., Ward, L. M., Mischna, M. A., & Fischer, W. W. (2019). Mars Extant life: What's next? *LPI Contributions*, 2108, 41550.
- Tung, H. C., Bramall, N. E., & Price, P. B. (2005). Microbial origin of excess methane in glacial ice and implications for life on Mars. *Proceedings of the National Academy of Sciences of the United States of America*, 102(51), 18292–18296. <https://doi.org/10.1073/pnas.0507601102>
- Viswanathan, G. M., Buldyrev, S. V., Havlin, S., Da Luz, M. G., Raposo, E. P., & Stanley, H. E. (1999). Optimizing the success of random searches. *Nature*, 401(6756), 911–914. <https://doi.org/10.1038/44831>
- Zimmerman, R. W., & Bodvarsson, G. S. (1996). Hydraulic conductivity of rock fractures. *Transport in Porous Media*, 23(1), 1–30.